Real-Time Diagnosis of Winding Axial Displacement in Power Transformers Using Time and Frequency Responses

[1]Milad Bandehzadeh, [2]Hamid Radmanesh *, [3]Payam Rabbanifar, [4]Shahram Javadi
[1]Department of Electrical Engineering,
Islamic Azad University Central Tehran Branch, Iran
E-mail: miladbandehzadeh@gmail.com
[2]Department of Electrical Engineering,
Islamic Azad University Central Tehran Branch, Iran
E-mail: h.radmanesh@iauctb.ac.ir
*Corresponding author
[3]Department of Electrical Engineering,
Islamic Azad University Central Tehran Branch, Iran
E-mail: pay.rabanifar@iauctb.ac.ir
[4]Department of Electrical Engineering,
Islamic Azad University Central Tehran Branch, Iran
E-mail: sh.javadi@iauctb.ac.ir

Article Received: 15 Sept 2024, Revised: 24 Oct 2024, Accepted: 04 Nov 2024

Abstract: The importance of a power transformer lies not only in its capital cost but also in the financial losses incurred due to the lack of supplied energy during its failure. Fault diagnosis in power transformers through online monitoring has gained significant attention over the past decade. The transfer function method has been increasingly employed for fault diagnosis in power equipment, particularly for detecting winding deformations in transformers. This paper investigates the online diagnosis of winding axial displacement in power transformers using time and frequency domain responses. The sensitivity of each method for detecting axial displacement is compared. Among the various criteria, the peak amplitude in the step response at the first extremum was selected as the most effective criterion, although other criteria showed slightly higher sensitivity. The monotonic variation of this criterion with respect to axial displacement played a significant role in this selection.

Keywords: Frequency Response, Online Fault Diagnosis, Power Transformer, Time Response, Transfer Function, Winding Axial Displacement.

Reference: to this paper should be made as follows: Milad Bandehzadeh, Hamid Radmanesh, Payam Rabbanifar and Shahram Javadi, Real-Time Diagnosis of Winding Axial Displacement in Power Transformers Using Time and Frequency Responses, Int J of Advanced Design and Manufacturing Technology, Vol. 2, No. 1, 2008, pp. 43–54.

Biographical notes: Author 1 received the B.Sc. degree from the Electrical Engineering Department,abbaspor (Beheshti university), Iran tehran .He received the M.Sc. degree from the Electrical Engineering Department, Islamic Azad University, Qazvin Branch, Iran and now PhD Candidate, Department of Electrical Engineering, Islamic Azad University Central Tehran Branch.

Author 2 Corresponding author received his Ph.D. degree in electrical engineering from Amirkabir University of Technology (AUT), Tehran. He has authored more than 100 published technical papers and has been involved in several industrial projects and educational programs in the fields of power electronics and power systems. His research interests include transient in power system, renewable energy, power quality, HVdc transmission systems, and more-electrical aircraft.

Author 3 received his PhD in Power Engineering from Elm o sanaat university. He is currently Professor at the Department of Elecrtical Engineering,Islamic Azad University Central Tehran Branch, Iran

Author 4 received his PhD in Power Engineering from Science and Research Branch. Tehran. He is currently Professor at the Department of Elecrtical Engineering,Islamic Azad University Central Tehran Branch, Iran

1 Introduction

A power transformer is one of the most crucial components in a power system [1]-[4]. Its significance extends beyond its capital cost, as the financial losses resulting from energy supply interruptions during transformer failures are considerable [1]-[2]. The failure of high-voltage transformers can cause irreparable damage to the entire power system [5]. Failures and defects in transformers can be categorized into three types: electrical, thermal, and mechanical. While electrical and thermal faults can be mitigated with appropriate monitoring and maintenance, mechanical defects often remain present in the transformer until the end of its operational life cycle. Electromagnetic forces acting on transformer windings, particularly during short circuit events (which can be 100 to 900 times greater than forces under rated load conditions), are a primary cause of winding deformation and, consequently, transformer failure [1]-[8]. Inrush currents, which occur more frequently and last longer than

Eksplorium *p*-ISSN 0854-1418
Volume 45 No. 2, November 2024: 300–310 *e*-ISSN 2503-426X

short circuit currents, also contribute to this issue [1]-[6]. Furthermore, during transportation to its installation site or in the event of an earthquake, winding deformation may also occur [9]-[11]. Over the past decade, fault diagnosis based on online monitoring has received significant attention. The adoption of more advanced diagnostic methods, however, introduces new challenges. Among the various advanced online methods for diagnosing winding deformation are transformer tank vibration analysis, ultrasonic testing, short circuit impedance measurements, transfer function analysis, and the use of leakage parameters [12]-[38]. Axial displacement or radial deformation of transformer windings, often caused by electromagnetic forces, is a critical issue [39]. Therefore, diagnosing axial displacement and radial deformation can be achieved using transfer function and short circuit impedance methods. Measuring the short circuit impedance of a transformer and comparing the obtained values with previous measurements or factory test results is an effective approach for diagnosing winding deformation. In other words, the short circuit impedance method relies on comparisons over time. This impedance is influenced by the transformer configuration and the distance between windings. A change in short circuit impedance of more than 3% in a transformer should be considered significant [36]. The transfer function method is widely used to describe the behavior of a system and has increasingly been employed in diagnosing power equipment faults, particularly winding deformations in transformers [37]-[38]. Various terminal conditions for measuring the transfer function of power transformers are illustrated in Fig. 1.

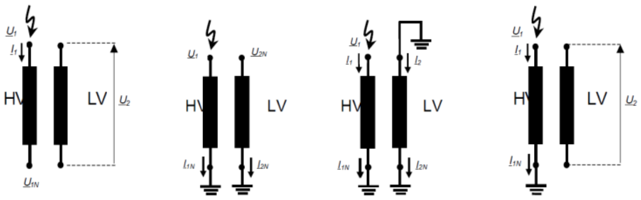

Fig. 1 Different terminal conditions for measuring the transfer function of a power transformer.

Faults such as short-circuited turns, mechanical damage to windings and the core, and loose turns can be detected using the transfer function method [40]-[43]. The high-frequency behavior of the windings is characterized by their resonances (transfer maxima) and transfer minima. Determining the exact location and severity of these faults remains an active area of research. This method is inherently comparative, meaning that the measurement results must be compared to reference values. If significant deviations are observed, it indicates a fault in the transformer, and appropriate corrective action must be taken [40]. The correlation between specific faults and the variations in the transfer function is not yet fully understood. These relationships can be established either through direct measurements on power transformers or by developing an appropriate model for simulation purposes [40].

A typical section of a detailed power transformer model is shown in Fig. 2 [42]. This figure illustrates in Fig. 2. This figure shows the i^{th} unit of the high voltage (HV) winding and the j^{th} unit of the low voltage (LV) winding, which contains self-inductance (L), mutual inductance (M), parallel capacitance of each unit (Kp), earth capacitance(Ce), capacitance between LV and HV windings (CHL), series resistance that represents the conductor ohmic losses of each unit (Rs), shunt resistance that represents dielectric losses (Rp) and insulation resistance between each unit and earth (tank or core) [42].

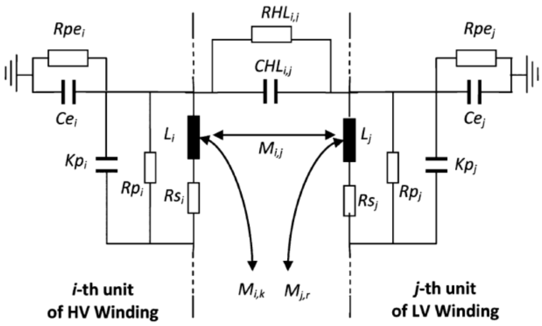

Fig. 2 A typical section of detailed model of the power transformer

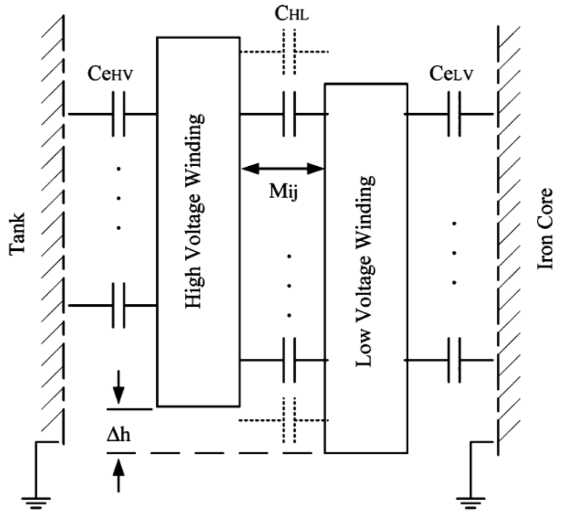

Fig. 3 Axial displacement of the HV winding with respect to the LV winding.

Axial displacement defects involve the axial movement of the high voltage (HV) winding relative to the low voltage (LV) winding, as shown in Fig. 3 [42]. This paper investigates the online diagnosis of winding axial displacement in power transformers using time and frequency responses. The sensitivity of each method for diagnosing axial displacement has been compared.

2 Transformer Specification

The specifications of the studied single-phase transformer are presented in Table 1. The HV winding is of the disk type, while the LV winding is of the layer type.

Table 1 Specification of the Transformer [43]

Parameter	Definition	Value	Unit
S_{rated}	Rated Apparent Power	1.6	MVA
$V_{rated,HV}$	Rated Voltage of High Voltage (HV) Winding	20	kV
$V_{rated,LV}$	Rated Voltage of Low Voltage (LV) Winding	0.4	kV
$N_{Disks,HV}$	Number of Disks in HV Winding	38	-
$N_{T, End\ Disks}$	Number of Turns in 8 Bottom and 8 Top Disks of HV Winding	20	-
$N_{T, Intermediate\ Disks}$	Number of Turns in 22 Intermediate Disks of HV Winding	21	-
$N_{Layers,LV}$	Number of Layers in LV Winding	2	-
$N_{T,Layers,LV}$	Number of Turns in each Layer of LV Winding	13	-

$N_{Paral. Cond., LV}$	Number of Paralleled Conductors in LV Winding	3	-
$R_{in, LV}$	Internal Radius of the LV winding	93	mm
$R_{out, LV}$	External Radius of the LV winding	106	mm
$D_{LV, Layers}$	Distance between the Layers of the LV winding	4	mm
$D_{LV, HV}$	Distance between the LV and HV windings	12.5	mm
$R_{in, HV}$	Internal Radius of the HV winding	118.5	mm
$R_{out, HV}$	External Radius of the HV winding	176.5	mm
$Cond._{LV,Dim}$	Dimensions of the LV Conductors	3.35 * 11.8	mm^2
$Cond._{HV,Dim}$	Dimensions of the HV Conductors	2.12 * 8.5	mm^2
W_{ins}	Thickness of the Insulation Paper	0.5	mm
H_{LV}	Height of the LV winding	536	mm
H_{HV}	Height of the HV winding	494	mm
R_{core}	Core Radius	90	mm

The transfer function of the studied transformer was determined using the system identification method outlined in [43]. The zeros, poles, and constant coefficient of the 16th-order transfer function for the healthy transformer, obtained using the system identification toolbox in MATLAB software with a 97.69% fit, are presented in Table 2. Additionally, the corresponding values for the transformer with 15, 30, 45, and 60 mm axial displacement of the winding are provided in Tables 3 through 6, respectively.

Table 2 Zeros, Poles, and Constant Coefficient of the 16th-Order Transfer Function of the Healthy Transformer [43]

oles ($*10^6$)	eros ($*10^6$)	t Coefficient (K)
219 ± j5.6952	001 ± j5.5288	$6274 * 10^{10}$
806 ± j3.9986	817 ± j3.7341	
562 ± j2.9719	520 ± j3.0027	
511 ± j2.3665	440 ± j1.8607	
335 ± j1.2686	336 ± j1.2934	
163 ± j0.7268	999 ± j0.7260	
137 ± j0.7058	71 ± j0.0000	
138 ± j0.5650	163 ± j0.5655	

Table 3 Zeros, Poles, and Constant Coefficient of the 16th-Order Transfer Function of the Transformer with 15 mm Axial Displacement [43]

oles (*10^6)	eros (*10^6)	t Coefficient (K)
945 ± j5.6837	859 ± j5.5355	.4952*10^{10}
563 ± j4.6225	627 ± j4.6457	
728 ± j3.9823	619 ± j3.7366	
606 ± j2.9423	613 ± j2.9759	
502 ± j2.3637	363 ± j1.8624	
287 ± j1.2681	285 ± j1.2922	
164 ± j0.7351	092 ± j0.0000	
002 ± j0.6010	002 ± j0.6019	

Table 4 Zeros, Poles and Constant Coefficient of the 16^{th} Order Transfer Function of the Transformer Considering 30 mm Axial Displacement [43]

Poles (*10^6)	Zeros (*10^6)	Constant Coefficient (K)
-0.1049 ± j5.6798	-0.0885 ± j5.5221	5.8040*10^{10}
-0.1835 ± j4.1648	-0.2246 ± j4.1451	
-0.0676 ± j3.9695	-0.0470 ± j3.7486	
-0.0625 ± j2.9315	-0.0646 ± j2.9696	
-0.0507 ± j2.3876	-0.0403 ± j1.8636	
-0.0284 ± j1.2732	-0.0282 ± j1.2988	
-0.0167 ± j0.7495	-0.0107 ± j0.0000	
-0.0011 ± j0.5722	-0.0010 ± j0.5720	

Table 5 Zeros, Poles, and Constant Coefficient of the 16th-Order Transfer Function of the Transformer with 45 mm Axial Displacement [43]

Poles (*10^6)	Zeros (*10^6)	Constant Coefficient (K)
-0.1267 ± j5.6611	-0.0956 ± j5.5012	6.5992*10^{10}
-0.0800 ± j3.9978	-0.0849 ± j3.7239	
-0.0493 ± j2.9378	-0.0443 ± j2.9764	
-0.0524 ± j2.4157	-0.0488 ± j1.8562	
-0.0314 ± j1.2851	-0.0280 ± j1.3132	
-0.0168 ± j0.7696	0.0156 ± j0.0000	
-0.3883 ± j0.3953	-0.3719 ± j0.4211	
-0.0431 ± j0.6018	-0.0494 ± j0.6036	

Table 6 Zeros, Poles, and Constant Coefficient of the 16th-Order Transfer Function of the Transformer with 60 mm Axial Displacement [43]

Poles (*10^6)	Zeros (*10^6)	Constant Coefficient (K)
-0.0983 ± j5.6776	-0.0907 ± j5.5380	6.8210*10^{10}
-0.0871 ± j4.6701	-0.0879 ± j4.6952	
-0.0731 ± j3.9989	-0.0653 ± j3.7295	
-0.0548 ± j2.9082	-0.0571 ± j2.9606	
-0.0531 ± j2.4604	-0.0350 ± j1.8567	
-0.0177 ± j0.7946	-0.0300 ± j1.3130	
-0.0293 ± j1.2861	-0.0027 ± j0.0000	
-0.1490 ± j0.1798	-0.1540 ± j0.1730	

3 Time And Frequency Responses

The step response, impulse response, and Bode diagram of the transfer function for the healthy transformer are presented in Figs. 4 to 6, respectively. These figures has been plotted using MATLAB, which is a very powerful tool for theses problems.

Limitations for this study are:

- nonlinearity has not been modeled.
- The effect of temperature change can not be examined.

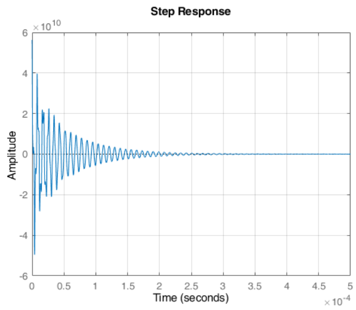

Fig. 4 Step response of the transfer function of the healthy transformer.

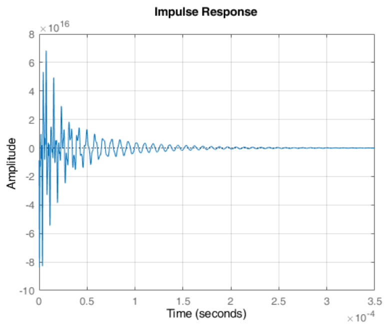

Fig. 5 Impulse response of the transfer function of the healthy transformer.

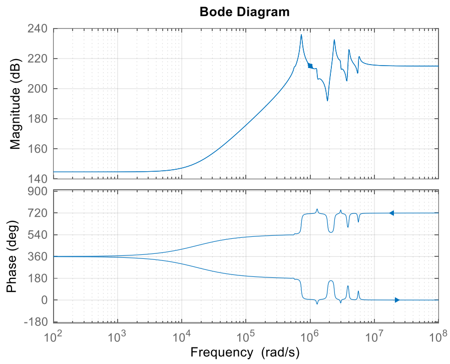

Fig. 6 Bode diagram of the transfer function of the healthy transformer.

The step response, impulse response, and Bode diagram of the transfer function for the healthy transformer and transformers with various axial displacement conditions are presented in Figs. 7 to 9, respectively.

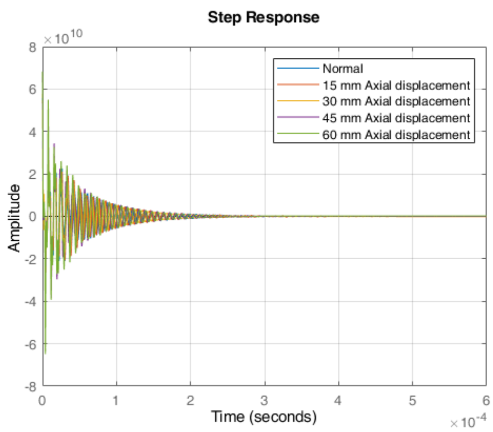

Fig. 7 Step response of the transfer function of the healthy transformer and transformer with other axially displaced winding condition.

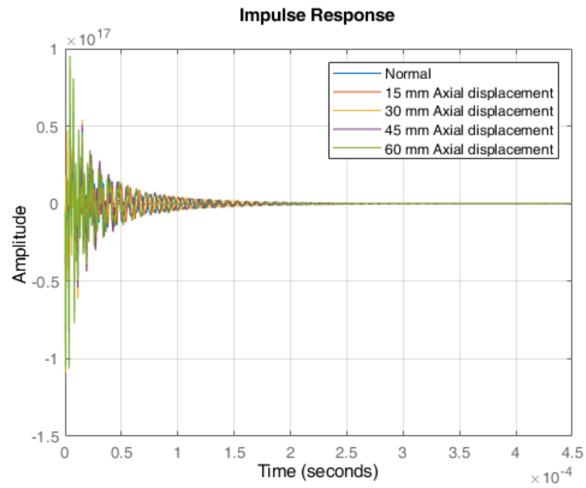

Fig. 8 Impulse response of the transfer function of the healthy transformer and transformer with other axially displaced winding condition.

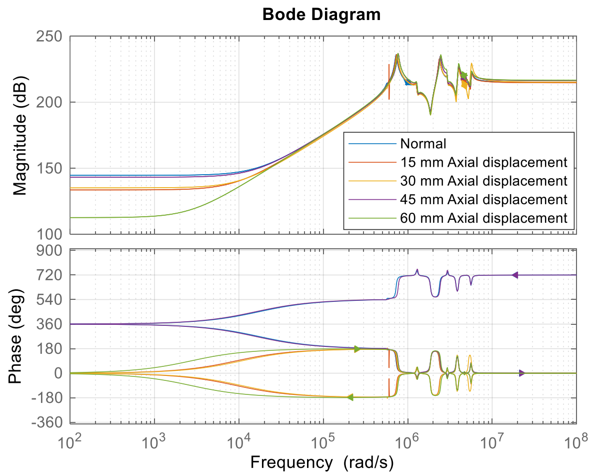

Fig. 9 Bode diagram of the transfer function of the healthy transformer and transformer with other axially displaced winding condition.

4 Discussion

Based on the results of the time and frequency responses presented in Section III, we can conclude the following:

- The sensitivity of the Bode diagram (frequency domain response) for detecting axial displacement is greater than that of the step and impulse responses (time domain responses).
- A significant difference in the magnitude (dB) of the Bode diagram at low frequencies is clearly observed in Table 7. The table shows that as the displacement increases, the magnitude (dB) decreases, although this reduction is not monotonic. The maximum percentage reduction occurs at the maximum displacement, which is 22.07%. The value of magnitude around the 100 rad/s is constant in each case and 100 rad/s is the lowest frequency which is considered in plot.
-

Table 7 Difference in the Magnitude of Bode Diagram at 100 rad/s

Condition	Magnitude (dB)	Percent of Change in Magnitude (dB) with respect to Healthy Case
Healthy	145	-
15 mm Axial Displacement	134	-7.59
30 mm Axial Displacement	135	-6.90

45 mm Axial Displacement	143	-1.38
60 mm Axial Displacement	113	-22.07

- The number of local extrema is the same in both the magnitude (dB) and phase (degrees) plots of the Bode diagram, except for one case with axial displacement (15 mm displacement). In the case of 15 mm axial displacement, two additional extrema appear around 6.01 × 10^5 rad/s and 6.02 × 10^5 rad/s. The magnitudes (dB) at these points are 228 dB and 202 dB, respectively. In other cases (excluding the 15 mm axial displacement), the average magnitude at these frequencies is 214 dB. Therefore, for the case with 15 mm axial displacement, the magnitudes at these two additional extrema show changes of 6.54% and -5.61%, respectively, compared to the average magnitude in the other cases.
- The peaks of the local extrema in both the magnitude and phase plots of the Bode diagram show slight differences when the windings are axially displaced. A comparison of the magnitude (dB) values at the first local maximum of the Bode diagram is presented in Table 8.

Table 8 Difference in the Magnitude of Bode Diagram at the First Local Maximum

Condition	Magnitude (dB)	Percent of Change in Magnitude (dB) with respect to Healthy Case
Healthy	235.9	-
15 mm Axial Displacement	236.2	0.13
30 mm Axial Displacement	235.5	-0.17
45 mm Axial Displacement	236.95	0.45
60 mm Axial Displacement	237.15	0.53

- The peak amplitudes of the step and impulse responses show a significant difference, while their settling times are nearly the same. The peak amplitudes at the first extremum of the step and impulse responses are presented in Tables 9 and 10. The peaks in the first extremums have the largest values with respect to other extremums.

Table 9 Difference in the Peak Amplitudes in the Step Response at Its First Extremum

Condition	Amplitude * 10^{10}	Percent of Change in Amplitude with respect to Healthy Case
Healthy	5.65	-
15 mm Axial Displacement	5.5	-2.65
30 mm Axial Displacement	5.8	2.65
45 mm Axial Displacement	6.6	16.81
60 mm Axial Displacement	6.85	21.24

Table 10 Difference in the Peak Amplitudes in the Impulse Response at Its First Extremum

Condition	Amplitude * 10^{16}	Percent of Change in Amplitude with respect to Healthy Case
Healthy	-8.3	-
15 mm Axial Displacement	-7.7	-7.23

30 mm Axial Displacement	-10.9	31.33
45 mm Axial Displacement	-10.2	22.89
60 mm Axial Displacement	-10.51	26.63

- All local extremums have been placed between 10^5-10^7 rad/s (15.9 kHz -1.59 MHz).

5 Conclusion

In this paper, the online diagnosis of winding axial displacement in power transformers using time and frequency responses has been investigated. The sensitivity of each method for diagnosing axial displacement has been compared. As discussed in the results section, the most sensitive criterion is the peak amplitude in the impulse response at its first extremum. The change in this criterion for the case with 30 mm axial displacement is 31.33% compared to the healthy case. It should be noted that the percentage change in this criterion is not monotonic with respect to the axial displacement. The second most sensitive criterion is the magnitude of the Bode diagram at 100 rad/s. The largest change in this criterion, occurring at 60 mm axial displacement, is -22.07% compared to the healthy case. However, like the previous criterion, the percentage change in this case is not monotonic with respect to axial displacement. The third most sensitive criterion is the peak amplitude in the step response at its first extremum. The change in this criterion for the 60 mm axial displacement case is 21.24% compared to the healthy case. The advantage of this criterion is its monotonic behavior with respect to axial displacement. Therefore, this criterion is considered the best for diagnosing axial displacement.

Competing Interests

The authors declare that they have no known financial or personal conflicts of interest that could have influenced the work reported in this paper.

References

[1] Kulkarni, S. V. and Khaparde, S. A., Transformer Engineering Design, Technology and Diagnostics, Marcel Dekker, 2004.
[2] Minhas, M. S. A., Dynamic Behaviour of Transformer Winding under Short-Circuits, PhD Dissertation, University of the Witwatersrand, 2007.
[3] Heathcote, M. J., The J&P Transformer Book, 13th ed, Elsevier, 2007.
[4] Moradnouri, A., Vakilian, M., Hekmati, A. and Fardmanesh, M., Optimal Design of Flux Diverter Using Genetic Algorithm for Axial Short-circuit Force Reduction in HTS Transformers, IEEE Transactions on Applied Superconductivity, Vol. 30, No. 1, pp. 1-8, 2020.
[5] Yousof Yousof, M. F., Frequency response analysis for transformer winding condition monitoring, MSc Thesis, The University of Queensland, 2015.
[6] Karsai, K., Kerenyi D., and Kiss L., Large Power Transformers, Elsevier, 1987.
[7] Moradnouri, A., Vakilian, M., Hekmati, A., and Fardmanesh, M., HTS Transformers Leakage Flux and Short-circuit Force Mitigation through Optimal Design of Auxiliary Windings, Cryogenics, Vol. 110, pp. 103148 2020.
[8] Flanagan, W. M., Handbook of Transformer Design &Applications, 2nd ed, McGraw-Hill, 1993.
[9] Zhou, L., Jiang, J., and Li, W., FRA modelling for diagnosing axial displacement of windings in traction transformers, IET Electric Power Applications, Vol. 13, No. 12, 2019.
[10] IEC Standard 60076-18 Ed. 1: Power transformers - Part 18, Measurement of frequency response, 2012.
[11] Shintemirov, A., Modeling and Condition Assessment of Power Transformers Using Computational Intelligence, PhD Dissertation. The University of Liverpool, 2009.
[12] Zhang, F., Ji, S., Shi, Y., and Zhu, L., Investigation on the Action of Eddy Current on Tank Vibration Characteristics in Dry-Type Transformer, IEEE Transactions on Magnetics, Vol. 55, No. 2, pp. 1-8, 2019.
[13] Garcia, B., Burgos J. C., and Alonso, A. M., Transformer tank vibration modeling as a method of detecting winding deformations-part I: theoretical foundation," in IEEE Transactions on Power Delivery, Vol. 21, No. 1, pp. 157-163, 2006.

[14] Garcia, B., Burgos J. C., and Alonso, A. M., Transformer tank vibration modeling as a method of detecting winding deformations-part II: experimental verification, IEEE Transactions on Power Delivery, Vol. 21, No. 1, pp. 164-169, 2006.
[15] He, T., Wang, J-Di., Guo, J., Huang, H., Chen, X. -X and Pan, J., A Vibration Based Condition Monitoring System for Power Transformers, Asia-Pacific Power and Energy Eng. Conf. (APPEEC), pp. 1-4, 2009.
[16] Hejazi, M.A., Choopani, M., Dabir M., and Gharehpetian, G.B., Effect of antenna position on online monitoring of transformer winding axial displacement using electromagnetic waves, IEEE 2nd Int. Power Energy Conf. (PECON), pp. 44-49, 2008.
[17] Akhavanhejazi, M., Gharehpetian, G. B., Faraji-Dana, R., Moradi, G.R., Mohammadi, M., and Alehoseini, H. A., A new on-line monitoring method of transformer winding axial displacement based on measurement of scattering parameters and decision tree, Expert Syst. Applications, Vol. 38, pp. 88868893, 2011.
[18] Hejazi, M. A., Gharehpetian, G. B., Moradi, G., Alehosseini, H. A., and Mohammadi, M., Online monitoring of transformer winding axial displacement and its extent using scattering parameters and k nearest neighbour method, IET Proc. Generation, Transmission Distribution, Vol. 5, pp. 824-832, 2011.
[19] Hang, T., Deswel, D., Dleon, F., An Online Data-Driven Technique for the Detection of Transformer Winding Deformations, IEEE Transactions on Power Delivery, Volume: 33, Issue: 2, 2018.
[20] Joshi P. M., and Kulkarni, S. V., A novel approach for online deformation diagnostics of transformer windings, IEEE Power and Energy Society, General Meeting, pp. 1-6, 2010.
[21] Zhang, Z., Qi, W., and Yuan, Z., Research on Multi-frequency Ultrasonic On-Line Monitoring Technology of Transformer Oil Based on Neural Network, China International Conference on Electricity Distribution (CICED), 2018.
[22] Yoa, C., Zhoa, Z., Chen, Y., and Zhoa, X., Transformer winding deformation diagnostic system using online high frequency signal injection by capacitive coupling, IEEE Transactions on Dielectrics and Electrical Insulation, Vol. 21 , Issue: 4, 2014.
[23] Gao, S.-b., and Wang, G., Study on on-line monitoring of windings deformation of power transformer, IEEE 8th Int'l. Conf. Developments in Power System Protection, pp. 335-338 Vol. 1, 2004.
[24] Hu, G., Zhang, L., Wu, X. Correia, D., and He, W., Detecting the Capacity of Distribution Transformer Based on an On-Line Method, Asia-Pacific Power and Energy Eng. Conf. (APPEEC), pp. 1-4, 2011.
[25] Palani, A., Santhi, S., Gopalakrishna S., and Jayashankar, V., Real Time Techniques to Measure Winding Displacement in Transformers During Short-Circuit Tests, IEEE Trans. Power Del., Vol. 23, pp. 726-732, 2008.
[26] Pan, J., Yan, X., Zhou H., Research on on-line monitoring of three-phase transformer winding deformation state based on short-circuit reactance, 12th IEEE Conference on Industrial Electronics and Applications, 2017.
[27] Luo, Y., Ye, J.; Gao, J., Wang, G., and Li, B., Recognition technology of winding deformation based on principal components of transfer function characteristics and artificial neural network, IEEE Transactions on Dielectrics and Electrical Insulation, Vol. 24, Issue 6, 2017.
[28] Zhoa, X., Yoa, C., Abu siada, A., Performance evaluation of online transformer internal fault detection based on transient overvoltage signals, IEEE Transactions on Dielectrics and Electrical Insulation, Vol. 24 , Issue: 6, 2017.
[29] Li, P., Zhang, B. G., Hao, Z. G, Hu, X. J. and Chu, Y. L., Research on Monitoring of Winding Deformation of Power Transformer by Online Parameter Estimation about Leakage Inductance, IEEE Int. Conf. Power Syst. Tech. pp. 1-6, 2006.
[30] Hao, Z. G., Zhang, B. H., Yan, C. G., Shao, B. R., Bo, X. F., and Z. Q., Research on integration of transformer protection and winding deformation detecting, IEEE Int. Conf. Power Syst. Tech. (POWERCON), pp. 1-8, 2010.
[31] Setayeshmehr, Borsi, H., Gockenbach E., and Fofana, I., Online monitoring of transformer via transfer function, IEEE Electr. Insul. Conf. (EIC), pp. 278-282, 2009.
[32] Nosratian, J., Seyedtabai, S., Gharepetian, G., Determination and localization of turn-to-turn fault in transformer winding using frequency response analysis, IET Science, Measurement & Technology, Vo. 12, Issue 3, 2018.
[33] Setayeshmehr, A., Fofana, I., Akbari, A., Borsi, H., and Gockenbach, E., Effect of temperature, water content and aging on the dielectric response of oil-impregnated paper, IEEE Int. Conf. Dielectr. Liquids (ICDL), pp. 1-4, 2008.

[34] Danielsen, S., Reconstruction of the Transformer Response from on-Line FRA Measurements Performed via Bushing Taps, Conference 2018 Condition Monitoring and Diagnosis (CMD).
[35] De Rybel, T., Singh, A., Vandermaar, J. A., Wang, M., Marti J. R. and Srivastava, K. D., Apparatus for Online Power Transformer Winding Monitoring Using Bushing Tap Injection, IEEE Trans. Power Del., Vol. 24, pp. 996-1003, 2009.
[36] Allan, D., Moore, H., Electric Power Transformer Engineering, CRC Press, USA, 2004.
[37] Florkowski, M., Exploitation stresses and challenges in diagnostics of electrical industrial equipment, IEEE Int. Sympos. Industrial Electronics (ISIE), pp. 15-25, 2011.
[38] Hashemnia N., Abu-Siada, A., and Islam, S. Improved power transformer winding fault detection using FRA diagnostics – part 1: axial displacement simulation , IEEE Transactions on Dielectrics and Electrical Insulation, Vol.: 22, Issue 1, 2015.
[39] Rahimpour, E., and Hamidi, N., The effects of axial displacement of transformer windings on impulse and transferred voltage distribution, Electric Power Systems Research, Vol. 76, Issues 6–7, 2006.
[40] Rahimpour, E., Christian, J., Feser, K., and Mohseni, H., Transfer function method to diagnose axial displacement and radial deformation of transformer windings, IEEE Transactions on Power Delivery, Vol. 18, No. 2, pp. 493-505, 2003.
[41] Ghanizadeh, A. J., Modeling and detection of axial displacement and radial deformation of power transformer winding using network transients, Amirkabir University of Technology (Tehran Polytechnic), 2014.
[42] Ghanizadeh, A. J., Gharehpetian, G. B, Application of Characteristic Impedance and Wavelet Coherence Technique to Discriminate Mechanical Defects of Transformer Winding, Electric Power Components and Systems, Vol. 41, No. 9, pp. 868-878, 2013.
[43] Karimifard, P., Gharehpetian, G. B., Ghanizadeh, A. J., and Tenbohlen, S., Estimation of simulated transfer function to discriminate axial displacement and radial deformation of transformer winding, COMPEL: The International Journal for Computation and Mathematics in Electrical and Electronic Engineering, Vol. 31, No. 4, pp. 1277-1292, 2012.